Journal of INTELLIGENT MATERIAL SYSTEMS and STRUCTURES
University of Maryland, College Park, Maryland 20742-3035 301-405-4111 jkresh@eng.umd.edu

# Composite materials stiffness determination and defects characterization using leaky Lamb wave (LLW) dispersion data

Yoseph Bar-Cohen[a], Ajit Mal[b], Shyh-Shiuh Lih[a] and Zensheu Chang[a]

[a] Jet Propulsion Laboratory, Caltech, MS 82-105, 4800 Oak Grove Dr., Pasadena, CA 91109-8099, 818-394-2610, fax 818-393-4057, yosi@jpl.nasa.gov

[b] Mechanical and Aerospace Engineering Department, University of California, Los Angeles, CA 90095

## ABSTRACT

The leaky Lamb wave (LLW) technique is approaching a maturity level that is making it an attractive quantitative NDE tool for composites and bonded joints. Since it was first observed in 1982, the phenomenon has been studied extensively, particularly in composite materials. The wave is induced by oblique insonification using a pitch-catch arrangement and the plate wave modes are detected by identifying minima in the reflected spectra to obtain the dispersion data. The wave behavior in multi-orientation laminates has been well documented and corroborated experimentally with high accuracy. The sensitivity of the wave to the elastic constants of the material and to the boundary conditions led to the capability to measure the elastic properties of bonded joints. Recently, the authors significantly enhanced the LLW method's capability by increasing the speed of the data acquisition, the number of modes that can be identified and the accuracy of the data inversion. In spite of the theoretical and experimental progress, methods that employ oblique insonification of composites are still not being applied as standard industrial NDE. The authors investigated the possible causes that are hampering the transition of the LLW to industrial application and identified 4 key issues. The current capability of the method and the nature of these issues are described in this paper.

**KEY WORDS**: Leaky Lamb Waves (LLW), NDE, Composites, Stiffness Constants, Plate Wave Modes

## INTRODUCTION

The high stiffness to weight ratio, low electromagnetic reflectance and the ability to embed sensors and actuators have made fiber-reinforced composites an attractive construction material for primary aircraft structures. These materials consist of fibers and a polymer matrix that are stacked in layers and then cured. A limiting factor in widespread use of composites is their high cost - composite parts are about an order of magnitude more expensive than metallic parts. The cost of inspection is about 30% of the total cost of acquiring and operating composite structures. This large portion of the total cost makes the need for effective inspection critical not only to operational safety but also to the cost benefit of these materials [Bar-Cohen, 1991]. Currently, there are several critical issues that are still challenging the NDE community with regards to inspection of composites. These issues include:

**Defect Detection and Characterization**: Composites are susceptible to the formation of many possible defects throughout their life cycle mostly due to the multiple step production process and their non-homogeneity with brittle matrix. These defects include delaminations, cracking, fiber fracture, fiber pullout, matrix cracking, inclusions, voids, and impact-damage. Table 1 lists some of the defects that may appear in composite laminates and their effect on structural performance. While the overall emphasis is on detection of delaminations, porosity and impact damage, Table 1 is showing that other defects can have a critical effect

on the performance of host structures. Therefore, it is essential to be able to characterize the hosted flaws in order to estimate their effect on the structural integrity.

**Material Properties Characterization**: Production and service conditions can lead to property degradation and sub-standard performance of primary structures. Causes for such degradation can be the use of wrong constituent (fiber or matrix), excessive content of one of the constituent (resin rich or starved), wrong stacking order, high porosity content, micro-cracking, poor fiber/resin interface aging, fire damage, and excessive environmental/ chemical/radiation exposure. Current destructive test methods of determining the elastic properties are using representative coupons. These methods are costly and they are not providing direct information about the properties of represented structures.

**Need for Rapid Large Area Inspection**: Impact damage can have critical effect on the structure capability to operate in service (see Table 1). This critical type of flaw can be induced during service life anywhere on the structure and it requires detection as soon as possible rather than waiting for the next scheduled maintenance phase. Repeated application of conventional NDE for verification of the structural integrity can be very expensive and takes aircraft out of their main mission. Since impact damage can appear anywhere, there is a need for a low-cost system that can be used to rapidly inspect large areas in field condition. The use of a robotic crawlers potentially can offer an effective approach [Bar-Cohen, 1997].

**Real-Time Health Monitoring**: A system of health-monitoring is needed to reduce the periodic inspection, which requires the temporary removal of the aircraft from service. Fundamentally, such health monitor systems emulate biological systems, where onboard sensors track the structural integrity throughout the life cycle. The life cycle starts from production and continues through service providing an alarm to indicate that a critical parameter was exceeded.

**Smart Structures**: The availability of compact actuators, sensors and artificial intelligence has made it possible to develop structures that self-monitor their own integrity and use actuators to avoid or timely respond to threats. The changing environment or conditions can be counteracted by adequate combination of actuators and sensors that change the conditions and/or dampen the threat. Artificial intelligence can be used to assure the application of the most effective response at the shortest time. An example of the application of smart structures is the reduction of vibrations that lead to fatigue.

**Residual Stresses**: Current state of the art does not provide effective means of nondestructive determination of residual stresses. Technology is needed to detect and relieve residual stresses in structures made of composite materials.

**Weathering and Corrosion Damage**: Composites that are bonded to metals are sensitive to exposure to service fluids, hygrothermal condition at elevated temperatures and to corrosion. Particular concern rises when aluminum or steel alloys are in a direct contact with graphite/epoxy or with graphite/polyimide laminates. The graphite, in graphite/epoxy composites, is cathodic to aluminum and steel and therefore the metal, which is either fastened or bonded to it, is eroded. In the case of graphite/epoxy the metal deteriorates, whereas in the case of graphite/polyimide defects are induced in the composite with the form of microcracking, resin removal, fiber/matrix interface decoupling and blister (e.g. delaminations). When an aluminum panel is coupled to a Gr/Ep protective coating the aluminum is subjected to a significant loss of strength. To prevent such degradation, a barrier layer is needed between the metal and the graphite/epoxy, where many times glass/epoxy or Kevlar/epoxy layers are used.

The level of degradation of composite materials exposed to service environment depends on the chemical structure of the polymer matrix. In thermoset composites, the epoxy absorbs moisture and loses its thermal stability as a matrix in a reversible plasticisation process. On the other hand, thermoplastics are susceptible to effects of aircraft fluids such as cleaning fluids, paint stripping chemicals and fuel. Imide polymers are sensitive to strong base producing amid acid salts and amides, and their degradation rate is determined by such parameters as the temperature, stress, and humidity. The strength of the material deteriorates at an exponential rate, however annealing can reduce the degradation rate.

TABLE 1: Effect of defects in composite materials

| Defect | Effect on the material performance |
|---|---|
| Delamination | Catastrophic failure due to loss of interlaminar shear carrying capability.<br>Typical acceptance criteria require the detection of delaminations that are ≥0.25-inch. |
| Impact damage | The effect on the compression static strength<br>• Easily visible damage can cause 80% loss<br>• Barely visible damage can cause 65% loss |
| Ply gap | Degradation depends on stacking order and location. For $[0,45,90,-45]_{2S}$ laminate:<br>- 9% strength reduction due to gap(s) in 0° ply<br>- 17% reduction due to gap(s) in 90° ply |
| Ply waviness | • Strength loss can be predicted by assuming loss of load-carrying capability.<br>• For 0° ply waviness in $[0,45,90,-45]_{2S}$ laminate, static strength reduction is:<br>- 10% for slight waviness<br>- 25% for extreme waviness<br>• Fatigue life is reduced at least by a factor of 10 |
| Porosity | • Degrades matrix dominated properties<br>• 1% porosity reduces strength by 5% and fatigue life by 50%<br>• Increases equilibrium moisture level<br>• Aggravates thermal-spike phenomena |
| Surface notches | • Static strength reduction of up to 50%<br>• Local delamination at notch<br>• Strength reduction is small for notch sizes that are expected in service |
| Thermal Over-exposure | Matrix cracking, delamination, fiber debonding and permanent reduction in glass transition temperature |

Generally, NDE methods are used to determine the integrity and stiffness of composite structures. While information about the integrity and stiffness can be extracted directly from NDE measurements, strength and durability can not be measured by such measurements because these are not physically measurable parameters. For many years, the multi-layered anisotropic nature of composites posed a challenge to the NDE research community. Pulse-echo and through-transmission are still the leading standard NDE methods of determining the quality of composites. However, these methods provide limited and mostly qualitative information about defects and material properties. The discovery of the leaky Lamb wave (LLW) [Bar-Cohen & Chimenti, 1984]

and the Polar Backscattering [Bar-Cohen & Crane, 1982] phenomena in composites enabled effective quantitative NDE of composites. These obliquely insonified ultrasonic wave techniques were studied both experimentally and analytically by numerous investigators [e.g., Bar-Cohen & Mal, 1988, Dayal & Kinra, 1991, and Nayfeh & Chimenti, 1988]. These studies led to the development of effective quantitative NDE capabilities for the determination of the elastic properties, to an accurate characterization of defects and even the determination of the quality of adhesively bonded joints [Bar-Cohen and Mal, 1989]. In spite of the progress that was made both theoretically and experimentally, oblique insonification techniques have not yet become standard industrial NDE methods for composite materials. The authors investigated the possible causes that are hampering the transition of these methods, particularly the LLW, to practical NDE. This manuscript covers the progress that was made in tackling the theoretical and experimental issues to the solidification of the foundation of the technique and the transition to practical NDE.

## LEAKY LAMB WAVE PHENOMENON

The phenomenon leaky Lamb wave (LLW) is induced when a pitch-catch ultrasonic setup is insonifies a plate-like solid immersed in fluid [Bar-Cohen, Mal and Lih, 1993]. This phenomenon was discovered by the principal author in August 1982 using Schlieren imaging system while testing a composite laminate (see Figure 1). The phenomenon is the result of a resonant excitation of plate waves that leak waves into the liquid coupling medium and interfere with the specular reflection. The LLW phenomenon is modifying the reflection spectrum introducing a series of minima associated with the related plate wave modes. These minima are the result of a destructive interference at the specific frequencies between the leaky and the spectral reflection. The LLW experimental procedure involves measurement of the reflections and extraction of the dispersive spectral characteristics at various angles of incidence and along several orientations with the laminate fibers. The data is presented in the form of dispersion curves showing the LLW modes phase velocity (calculated from Snell's law and the angle of incidence) as a function of the frequency.

Following the LLW discovery, a joint study was conducted by [Bar-Cohen and Chimenti, 1984] who investigated the characteristics of the LLW phenomenon and its application to NDE. These two investigators concentrated on the experimental documentation of observed modes and the effect of defects. Their study was followed by numerous other investigations of the phenomenon [e.g., Mal & Bar-Cohen, 1988, Dayal & Vikram, 1991, and Nayfeh & Chimenti, 1988]. In 1987, [Mal, 1988] developed a model that can be used to accurately predict the wave behavior. The results were corroborated experimentally and then a method was developed to invert the elastic properties using the LLW dispersion data [Mal & Bar-Cohen, 1988]. This study was later expanded to NDE of bonded joints [Bar-Cohen & Mal, 1989].

The experimental acquisition of dispersion curves for composite materials requires accurate control of the angle of incidence/reception and the polar angle with the fibers. The need to perform these measurements rapidly and accurately was effectively addressed at JPL where a specially designed LLW scanner was developed [Bar-Cohen, Mal & Lih, 1993]. With the aid of a personal computer, this scanner controls the height, angle of incidence and polar angle of the pitch-catch setup. The LLW scanner controls the angle of incidence/reception simultaneously while maintaining a pivot point on the part surface. A view of the LLW scanner installed on a C-scan unit is shown in Figure 2. A computer code was written to control the incidence and polar angles, the height of

the transducers from the sample surface, and the transmitted frequency. In prior studies, the data acquisition involved the use of sequentially transmitted tone-bursts at single frequencies over a selected frequency range (within the 20dB level of the transducer pair). Reflected signals are acquired as a function of the polar and incidence angle and are saved in a file for analysis and comparison with the theoretical predictions. The minima in the acquired reflection spectra represent the LLW modes and are used to determine the dispersion curves (phase velocity as a function of frequency). The incident angle is changed incrementally within the selected range and the reflection spectra are acquired. For graphite/epoxy laminates the modes are identified for each angle of incidence in the range of 12° to 50° allowing the use of free-plate theoretical calculations. At each given incidence angle, the minima are identified and are added to the accumulating dispersion curves, and are plotted simultaneously on the computer display. While the data acquisition is in progress, the acquired minima are identified on both the reflection spectra and the dispersion curves.

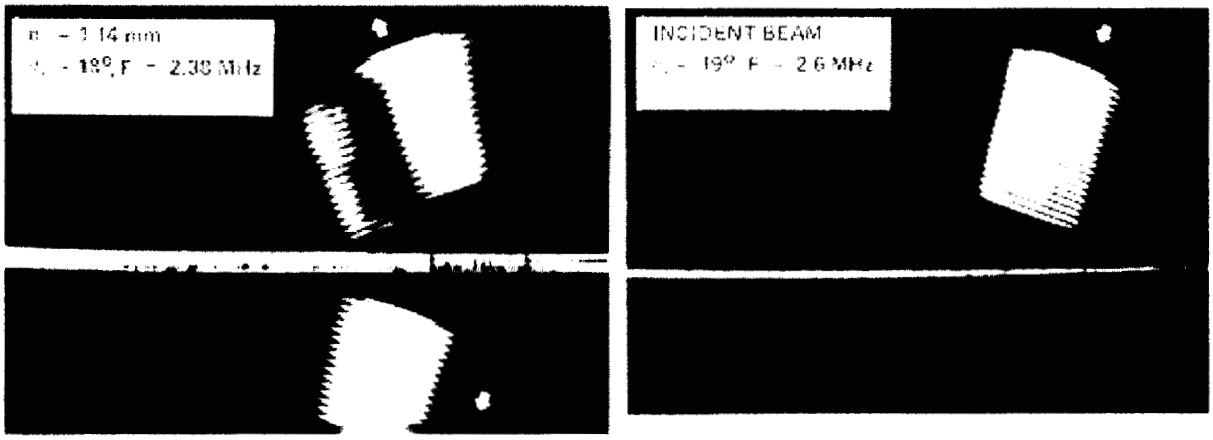


FIGURE 1: A Schlieren image of the LLW phenomenon showing a tone-burst before and after impinging on the graphite/epoxy laminate.

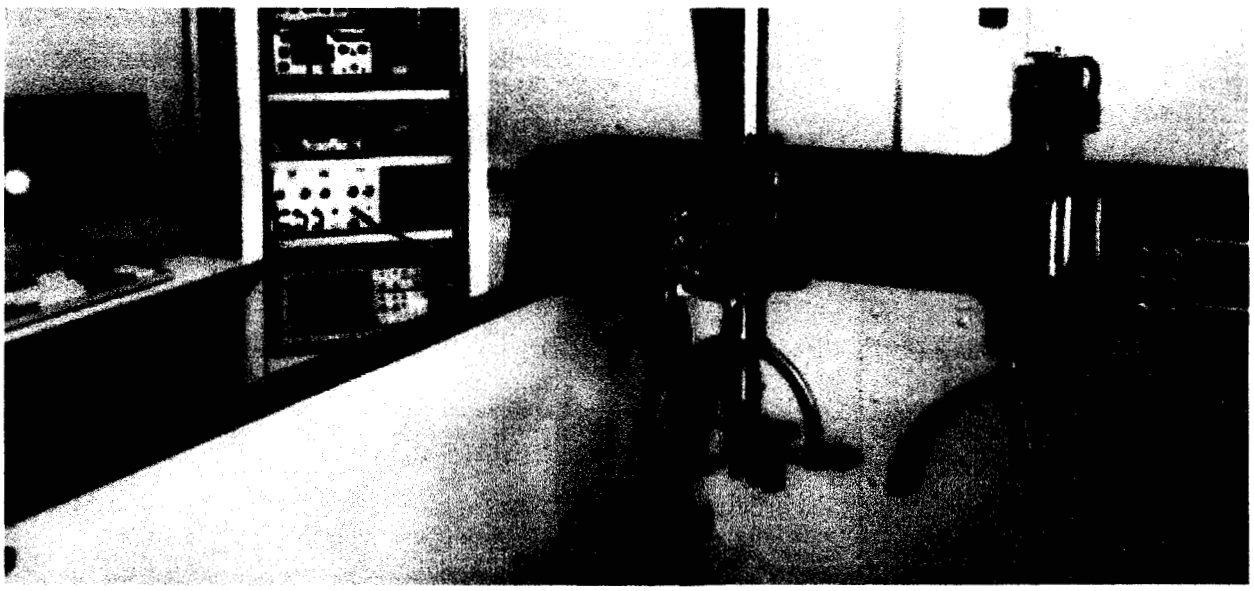

FIGURE 2: A view of the LLW scanner (bridge right side) installed on the JPL's C-scan system

A follow-on study by [Bar-Cohen, Mal & Lih 1993] showed that the capability to invert the elastic properties using LLW data is limited to the matrix dominated ones. To overcome this limitation, which is associated with the need for angles of incidence as small as 8°, a methodology was developed that is based on using ultrasonic pulses. Assuming that the material is transversely isotropic and using pulses in pitch-catch and pulse-echo experimental arrangements, it was shown that all the five elastic constants can be determined fairly accurately. A parametric study was conducted and the expected error was determined for the various determined constants in relation to experimental errors. It was also shown that, $C_{12}$, the constant with the most sensitivity to defects, is critically sensitive to alignment errors in the incident and polar angles.

## LLW THEORY AND DATA INVERSION

### Plate wave theory

The behavior of an ultrasonic wave, which is propagating through a composite material, is determined by the material stiffness matrix and the wave attenuation. To determine this behavior several assumptions can be made about fiber reinforced composite materials. The material can be treated as homogeneous since the fiber diameter (e.g., graphite 5-10μm and glass 10-15μ) is significantly smaller than the wavelength (for frequencies up to 20 MHz the wavelength is larger than 100μ). Each layer is assumed transversely isotropic bonded with a thin layer of an isotropic resin. The mechanical behavior of an individual lamina is described by an average of the displacements, the stresses and the strains over representative elements. The average strains are related to the average stresses through the effective elastic moduli. As a transversely isotropic material, unidirectional fiber-reinforced composites are characterized by five independent effective stiffness constants. These constants dependent on the elastic properties of the fiber and matrix materials as well as their volume fraction. The stress components of the wave are related to the strain through a linear constitutive equation. For a transversely isotropic elastic solid with its symmetry axis along the $x_1$-axis (along to the laminate) this equation can be expressed in the form [Christensen, 1981]

$$\begin{Bmatrix} \sigma_{11} \\ \sigma_{22} \\ \sigma_{33} \\ \sigma_{23} \\ \sigma_{31} \\ \sigma_{12} \end{Bmatrix} = \begin{bmatrix} c_{11} & c_{12} & c_{12} & 0 & 0 & 0 \\ c_{12} & c_{22} & c_{23} & 0 & 0 & 0 \\ c_{12} & c_{23} & c_{22} & 0 & 0 & 0 \\ 0 & 0 & 0 & c_{44} & 0 & 0 \\ 0 & 0 & 0 & 0 & c_{55} & 0 \\ 0 & 0 & 0 & 0 & 0 & c_{55} \end{bmatrix} \begin{Bmatrix} u_{1,1} \\ u_{2,2} \\ u_{3,3} \\ u_{2,3}+u_{3,2} \\ u_{1,3}+u_{3,1} \\ u_{1,2}+u_{2,1} \end{Bmatrix}$$

where $\sigma_{ij}$ is the Cauchy's stress tensor, $u_i$ is the displacement components, $c_{44} = (c_{22} - c_{23})/2$ and the five independent stiffness constants of the material are $c_{11}$, $c_{12}$, $c_{22}$, $c_{23}$ and $c_{55}$.

Modeling the effective elastic moduli of composite materials has been the topic of many studies. Extensive discussions of the bounds for the effective elastic moduli of fiber-reinforced composites can be found in [Christensen, 1981] and other associated literature cited therein. For low frequencies and low fiber concentration, the theoretical prediction of the effective elastic constants is in good agreement with experimental results. On the other hand, for high frequencies the theoretical estimates are not satisfactory since the effect of wave scattering by the fibers becomes significant. For fiber-reinforced composite materials, dissipation of the waves is

caused by the viscoelastic nature of the resin and by multiple scattering from the fibers as well as other inhomogeneities. Both dissipation effects can be modeled by assuming complex and frequency-dependent stiffness constants, $C_{ij}$.

The interaction of ultrasonic waves obliquely insonifying a composite plate excites various elastic wave modes. These modes are strongly affected by the material integrity as well as the bulk and interface properties. The material characteristics can be extracted from the reflected and transmitted acoustic data that is acquired as a function of frequency and angle of incidence. A pitch-catch setup is assumed to be immersed in water insonifying a fiber-reinforced plate by a plane harmonic acoustic wave. To formulate the wave field a modified form of the potential function method described in [Buchwald, 1961] is applied here.

For the formulation of the model, the displacement vector $\{u_1, u_2, u_3\}$ is expressed in terms of three scalar potentials $\Phi_j$ ($j = 1, 2, 3$) as follows

$$u_1 = \frac{\partial \Phi_1}{\partial x_1}$$

$$u_2 = \frac{\partial \Phi_2}{\partial x_2} + \frac{\partial \Phi_3}{\partial x_3}$$

$$u_3 = \frac{\partial \Phi_2}{\partial x_3} - \frac{\partial \Phi_3}{\partial x_2}$$

A sufficient condition for the displacements to satisfy Cauchy's equations of motion is that the potential satisfies the following differential equation.

$$\begin{bmatrix} a_5\nabla_1^2 + a_2\dfrac{\partial^2}{\partial x_1^2} + \omega^2 & a_3\nabla_1^2 & 0 \\ a_2\dfrac{\partial^2}{\partial x_1^2} & a_1\nabla_1^2 + a_5\dfrac{\partial^2}{\partial x_1^2} + \omega^2 & 0 \\ 0 & 0 & a_5\dfrac{\partial^2}{\partial x_1^2} + a_4\nabla_1^2 + \omega^2 \end{bmatrix} \begin{Bmatrix} \Phi_1 \\ \Phi_2 \\ \Phi_3 \end{Bmatrix} = \{0\}$$

where $\nabla_1^2 = \partial^2/\partial x_2^2 + \partial^2/\partial x_3^2$. This equation gives a partially decoupled system of differential equations for the potentials. The general solution of these equations is in the form of plane waves with wavenumbers $\xi_1$, $\xi_2$ along the $x_1$ and $x_2$ directions may be expressed as

$$\begin{Bmatrix} \Phi_1 \\ \Phi_2 \\ \Phi_3 \end{Bmatrix} = \begin{bmatrix} q_{11} & q_{12} & 0 \\ q_{21} & q_{22} & 0 \\ 0 & 0 & 1 \end{bmatrix} \{D\} e^{i(\xi_1 x_1 + \xi_2 x_2)}$$

where

$$\{D\} = Diag[e^{i\zeta_1 x_3}, e^{i\zeta_2 x_3}, e^{i\zeta_3 x_3}]\{C^+\} + Diag[e^{-i\zeta_1 x_3}, e^{-i\zeta_2 x_3}, e^{-i\zeta_3 x_3}]\{C^-\}$$

and the unknown vectors $\{C^+\} = \{C_1^+\ C_2^+\ C_3^+\}$ and $\{C^-\} = \{C_1^-\ C_2^-\ C_3^-\}$. The "vertical" wavenumbers $\zeta_j$ ($j$ = 1, 2, 3) and the factors $q_{ij}$ ($i$, $j$ = 1, 2) are dependent on the material symmetry. Definition of $\zeta_j$ and $q_{ij}$ can be found in [Mal, Yin, & Bar-Cohen, 1991].

We assume that the incident ray is inclined at angle $\theta$ to the $x_3$-axis and that the plane containing the incident ray and the $x_3$-axis is rotated at angle $\varphi$ to the $x_1$-axis. Let $\alpha_0$ be the acoustic wave speed in water and $\rho_0$ is the density of water. Then, the wave field due to the incident wave must be of the form $e^{i(\xi_1 x_1 + \xi_2 x_2 + \zeta_0 x_3)}$, where $\xi_1 = k_0 \sin\theta \cos\varphi$, $\xi_2 = k_0 \sin\theta \sin\varphi$, $\zeta_0 = k_0 \cos\theta$, and $k_0 = \omega/\alpha_0$. The plane acoustic waves in the fluid can be represented in terms of two Helmholz potentials, $\Phi_0$ for the upper fluid and $\Phi_b$ for the lower fluid. The displacement and stress components in the acoustic field are given by

$$u_i = \partial \Phi_\alpha / \partial x_i$$
$$\sigma_{33} = -\rho_0 \omega^2 \Phi_\alpha$$
$$\sigma_{13} = \sigma_{23} = 0$$

where $\alpha$ = 0 or b, represents for the fluid field above or under the plate, respectively.

For an ideal fluid, the shear stress components vanish. At the fluid-solid interfaces, the normal component of displacement is continuous, however, a tangential slip between the fluid and the solid is allowed. Thus, the boundary conditions at the top and bottom surfaces of the plate can be expressed in the form

$$S(x_3) = \left\{U_0,\ V_0,\ \Phi_{0,3},\ 0,\ 0,\ -\rho_0,\ \omega^2,\ \Phi_0\right\},\ x_3 = 0$$
$$= \left\{U_1,\ V_1,\ \Phi_{b,3},\ 0,\ 0,\ -\rho_0,\ \omega^2,\ \Phi_b\right\},\ x_3 = H$$

where $U_0$, $V_0$ and $U_1$, and $V_1$ are the components of the slip on the tangential plane at $x_3$ = 0 and $H$, respectively.

For an $N$ layered composite laminate, the vector $\{S_m(x_3)\}$ each layer each layer can be represented by constants $A_m^{\pm}$ as the same form in above equation. Then the field equations incorporate the prescribed conditions at the two fluid-solid interfaces and the continuity conditions at the inner interfaces can be solved by a global matrix method suggested by [Mal, 1988].

**Simplex Algorithm**

The locations of the minima in the reflection coefficients are highly sensitive to the thickness and the stiffness constants of the plate and are insensitive to the damping parameters as well as the presence of water in a broad frequency range. Thus the dispersion data can, in principle, be used to determine accurately these properties and any changes in their values during service. The phase velocity of guided waves in a composite laminate in absence of water loading is obtained from the theoretical model as a transcendental equation and its function requires minimization. The minimization can be carried out through a variety of available optimization schemes; we have used

the Simplex algorithm. The Simplex algorithm is a curve-fitting algorithm capable of fitting a set of data points to any function, no matter how complex it is. To illustrate how the algorithm works, let's start with a simple example. A function $f$ has two variables $x$ and $y$, and two unknown constant parameters $a$ and $b$ as shown below,

$$f(a,b;x,y)=0$$

There are totally $n$ sets of data $x_i$, $y_i$, $i$ = 1 to $n$. Each set of the data points substituted into the function $f$ yields

$$\varepsilon_i = f(a,b;x_i,y_i)$$

Define a new function as

$$S=\sum_{i=1}^{n} w_i \cdot \varepsilon_i$$

where $w_i$ is a statistical weight. Now, the problem of curve fitting becomes the problem of finding a set of the unknown parameters $a$ and $b$ that gives the minimum value of the function $S$.

A simplex algorithm can be described as a geometric figure (see Figure 3) that has one more vertex than the space in which it is defined has dimensions. For example, a simplex on a plane (a two-dimensional space) is a triangle; a simplex in a three-dimensional space is a tetrahedron, and so on. Returning back to the previous example, we build a plane with $a$ and $b$ as the two axes; then create a simplex (a triangle) as shown in the Figure 3. Each vertex of the triangle is characterized by three values: $a$, $b$ and $S$.

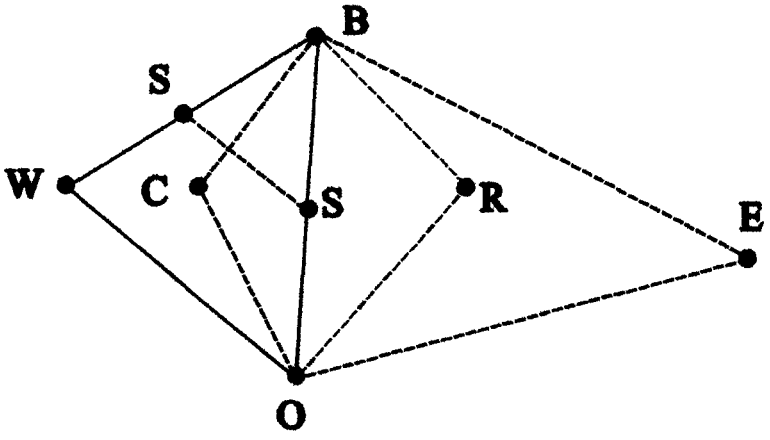


FIGURE 3: A 2-D simplex BWO illustrating the four mechanisms of movement: reflection, expansion, contraction, and shrinkage. B = best vertex, W = worst vertex, R = reflected vertex, E = expanded vertex, C = contracted vertex, and S = shrinkage vertexes.

To reach the minimum value of $S$, the following rules are used: find which vertex has the highest (worst) response and which has the lowest (best), then reject the highest and substitute another one for it. Four mechanisms are used to find the new vertex: reflection, expansion, contraction, and shrinkage. Call $d$ the distance from the worst vertex to $M$, the midpoint of all the other vertexes. The reflected vertex is located at a distance $d$ from $M$ on the line continuation that joins the rejected vertex to $M$. The response of the reflected vertex is calculated and compared to the responses of previous set of vertexes. The results can be divided into three groups as follow:

- The reflected vertex has a lower (better) response than the previous best. Then the expanded vertex (by reflecting twice the distance $d$) is tested. The expanded vertex is accepted if it has a lower response than the rejected one; otherwise the reflected one is accepted.

- The reflected vertex has a higher (worse) response than the rejected vertex. Then the contracted vertex (by moving the rejected one a distance of one-half $d$ toward the midpoint $M$) is tested. This contracted vertex is accepted if it produces a better (lower) response than the rejected one; otherwise, a shrinkage occurs and all vertexes, except the best one, move directly toward it by half of their original distance from it.
- The reflected vertex has a response better than the rejected one and worse than the best one. Then this reflected vertex is accepted.

These four mechanisms are illustrated in the Figure 3. The above steps are repeated until satisfied convergence is achieved. The locations of the minima in the reflection coefficients are highly sensitive to the thickness and the stiffness constants of the plate and are insensitive to the damping parameters as well as the presence of water in a broad frequency range. Thus the dispersion data can, in principle, be used to determine accurately these properties and any changes in their values during service. The phase velocity of guided waves in a composite laminate in absence of water loading is obtained from the theoretical model as a transcendental equation of the form,

$$G(\mathrm{v}, f, c_{ij}, H) = 0$$

For a given data set $\{f_k, v_k\}$, $c_{ij}$ and $H$ can be determined by minimizing the objective function

$$F(c_{ij}, H) = \Sigma\, w_k |\, G_k\,|^2$$

where $w_k$ is a suitable weight function and $G_k$ is the value of the dispersion function $G$ at the k-th data set.

**Experimental corroboration of the inversion model**

The inversion of the dispersion curves using the inversion equation is strongly nonlinear in $c_{ij}$ (stiffness matrix) and $H$ (thickness), and its solution is non-unique. Thus, extreme care must be taken in interpreting the numerical results obtained from the inversion of the dispersion data. Extensive parametric studies of the inversion process showed that only the thickness and the matrix dominated constants $c_{22}$, $c_{23}$ and $c_{55}$ can be determined accurately from the inversion of the dispersion data. The fiber dominated constants, $c_{11}$ and $c_{12}$, can be determined from the travel times and amplitudes of reflected short-pulse signals in an oblique insonification experiment [Bar-Cohen, Mal and Lih 1993].

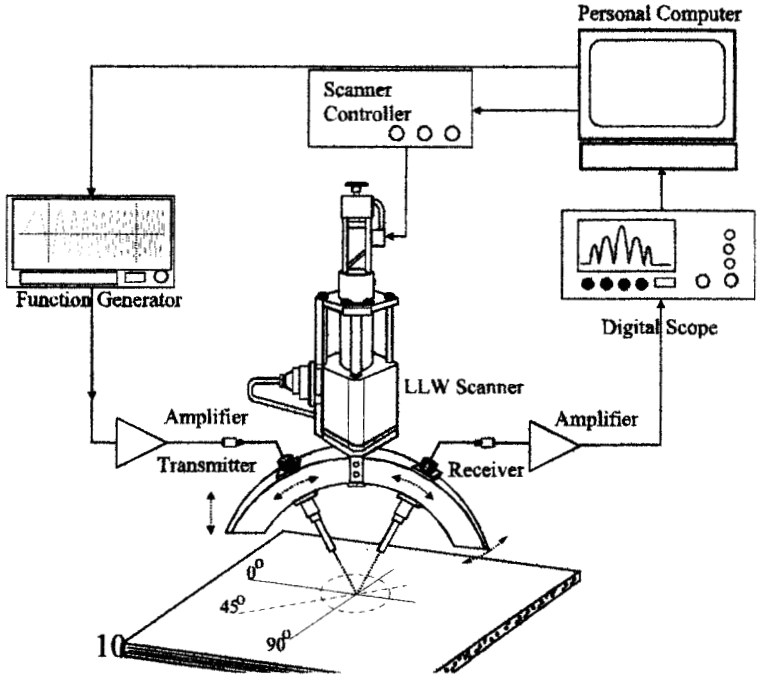


FIGURE 4: A schematic view of the rapid LLW test system.

This system consists of a LLW scanner (center of Figure 4) which is computer controlled to allow changing the transducers' height, rotation angle and the angle of incidence. The LLW scanner is an attachment add-on to ultrasonic scanning systems and is shown photographically in Figure 2. The control of the angle of incidence allows simultaneous change of the transmitter and receiver angle while maintaining a pivot point on the part surface and assuring accurate measurement of the reflected ultrasonic signals. The signals are transmitted by a function generator that FM modulates the required spectral range. This generator also provides a reference frequency marker for the calibration of the data acquisition when converting the signal from time to frequency domain. A digital scope is used to acquire the reflection spectral data after being amplified and rectified by an electronic hardware. The signals that are induced by the transmitter are received, processed and analyzed by a personal computer after being digitized. As discussed earlier, the reflected spectra for each of the desired angles of incidence is displayed on the monitor and the location of the minima (LLW modes) are marked by the computer on the reflection spectrum. These minima are accumulated on the dispersion curve, which is shown on the lower part of the display (see Figure 5). The use of the FM modulation approach enabled a significant increase in the speed of acquiring dispersion curves. 20 different angles of incidence were acquired in about 45 seconds as oppose to over 15-minutes using the former approach. Once the dispersion data is ready, the inversion option of the software is activated and the elastic stiffness constants are determined as shown in Figure 5.

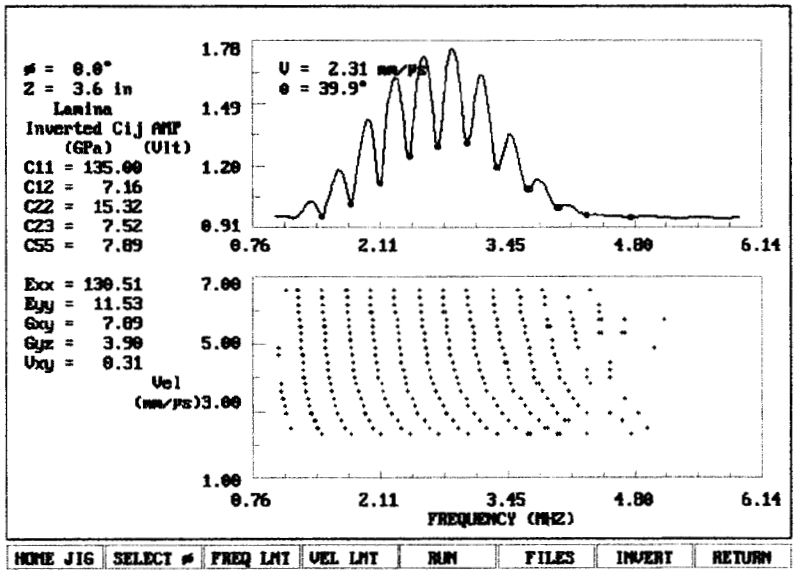


FIGURE 5: Computer display after the data acquisition and inversion completion. The elastic stiffness constants are inverted from the dispersion curve and are presented on the left of the screen.

Using the system with the enhanced data acquisition speed, various defects can be detected and characterized based on the signature and quantitative data that is available from the dispersion curves. In Figure 6a, the response from a defect-free graphite/epoxy laminate tested at the 0-degree polar angle is shown. In Figure 6b, the response from an area with a layer of simulated porosity (microballoons) is presented. As expected, at low frequencies the porosity has a relatively small effect and the dispersion curve appears similar to the one on Figure 6a. On the

other hand, as the frequency increases, the porosity layer emulates a delamination and modifies the dispersion curve to appear the same as half the thickness laminate.

**Experimental Data and Application of Simplex Inversion**

Typical LLW dispersion data and inverted results for a unidirectional graphite/epoxy plate was shown in Figure 5. The material is AS4/3501-6 and the polar angle (i.e., the direction of Lamb wave propagation) is 0°. The reflected spectrum for 39.9° incident angle is shown at the top of this Figure, and the accumulating dispersion curves are at the bottom. The inverted elastic and stiffness constants are given at the left. To demonstrate the capability of the LLW method to characterize materials degradation of composites, a sample made of AS4/3501-6 $[0]_{24}$ laminate was tested after it was subjected to heat treatment. The sample was exposed to a heat ramp from room temperature to 480° F for 15 minutes, and then was taken out of the oven to cool in open air at room temperature. The sample was tested at a specific location before and after heat treatment. The measured dispersion curves are shown in Figure 7. It can be seen that there are distinct differences in the dispersion data for the specimen before and after heat treatment. Since the heat damage occurs mostly in the matrix, the effect is expected to be more pronounced in the matrix dominated stiffness constants. The constants $c_{11}$, $c_{12}$, $c_{22}$, $c_{23}$ and $c_{55}$ obtained from the inversion process are 127.9, 6.32, 11.85, 6.92 and 7.43 GPa, before heat treatment, and 128.3, 6.35, 10.55, 6.9 and 7.71 GPa, after heat treatment. The most noticeable and significant change is in the stiffness constant $c_{22}$, which is the property most sensitive to variations in the matrix resulting in a reduction in the transverse Young's modulus.

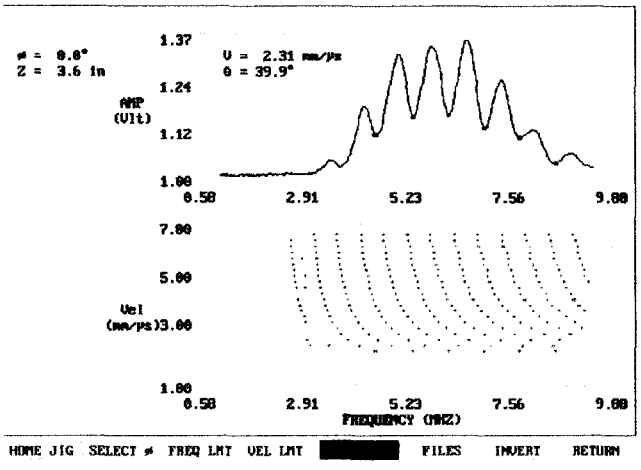


FIGURE 6a: The refection at 39.5 degrees incidence angle and the dispersion curve for a Gr/Ep $[0]_{24}$ laminate with no defects

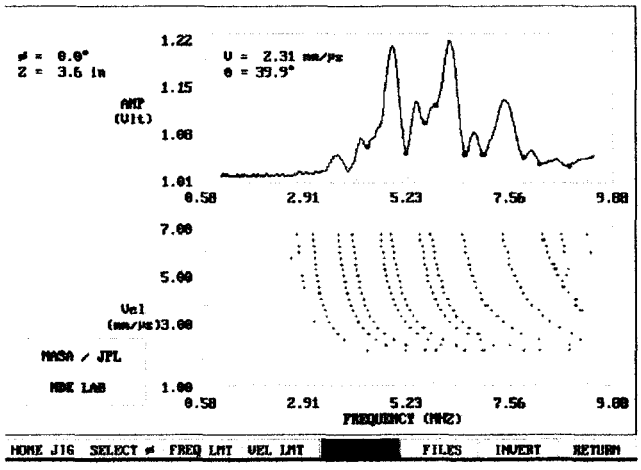


FIGURE 6b: The response at a defect area where porosity was simulated in the middle layer.

It should be noted that the inversion equation is strongly nonlinear in $c_{ij}$ and $H$, and its solution is non-unique. Thus, extreme care must be taken in interpreting the numerical results obtained from the inversion of the dispersion data. On the basis of extensive parametric studies of inversion equation, it has been concluded that only the thickness and the matrix dominated constants $c_{22}$, $c_{23}$ and $c_{55}$ can be determined accurately from the inversion of the dispersion data. This is due to the fact that the dispersion function G is not very sensitive to the fiber dominated constants $c_{11}$ and $c_{12}$. These two constants can be determined accurately from the travel times and amplitudes of the reflected short-pulse signals in the oblique insonification experiment. The

composite is modeled as a transversely isotropic and dissipative medium and the calculated dispersion curves are compared to the experimental data using the LLW setup.

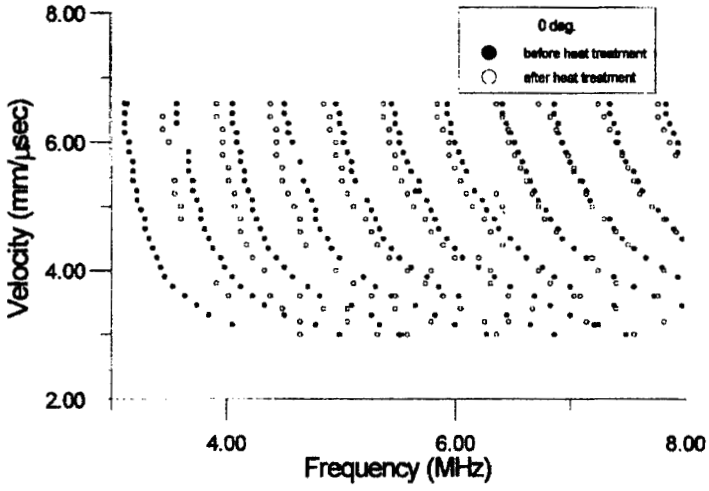


FIGURE 7: The measured dispersion curves of a $[0]_{24}$ graphite-epoxy panel before and after heat treatment.

**RAPID IDENTIFICATION OF MODES IN THE SCANNED DISPERSION CURVE**

To enhance the accuracy of the inversion of the material stiffness constants, a method was developed to acquire dispersion curves and display them in a graphics format as shown in Figure 8. This method allows viewing modes with amplitude levels that are significantly smaller than those observed previously. The bright curved lines show the modes in the background of the reflected spectra. Methods of extracting the modes were investigated using image processing operators and neural network procedures. Once the curve of a specific mode is determined, it is transformed to actual frequency vs. velocity data and then inversion is applied. This process involves a trade-off between noise suppression and localization, where an edge detection operator is used to reduce noise but it adds uncertainty to the location of the modes. Our approach consisted of using a linear operator that employs a first derivative Gaussian filter. This filter numerically approximated standard finite-difference for the first partial derivatives in the x and y directions. This type of operator is not rotationally symmetric and it is sensitive to the edge in the direction of steepest change, but acts as a smoothing operator in the direction along the edge.

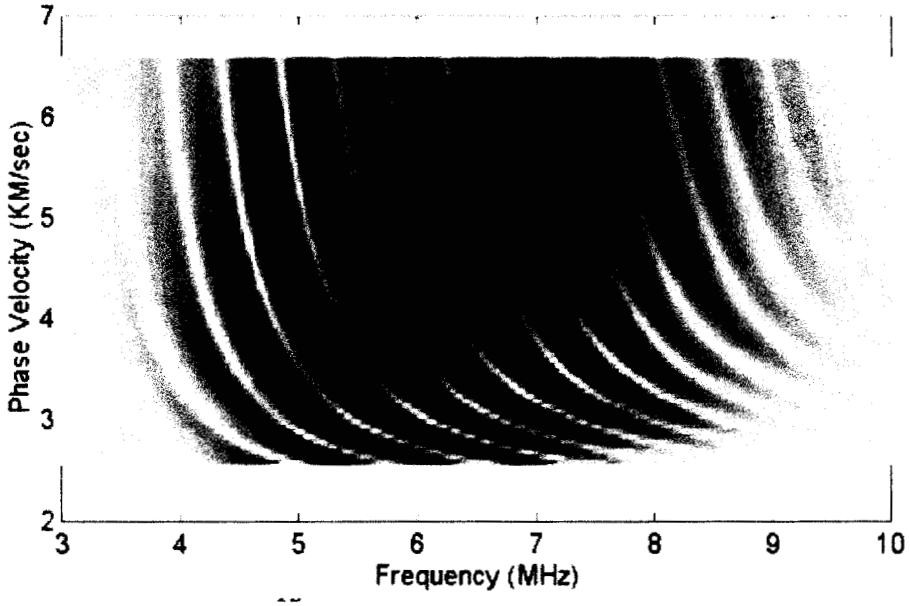


FIGURE 8: A view of an imaging method of presenting LLW dispersion curve.

## MULTIPLEXED LLW SYSTEM

The basic setup of a typical LLW data acquisition system was shown in Figure 2, where the angle of a pair of transducers is physically changed in steps. This motion places a practical limit on the speed of dispersion data acquisition, which has been in the range of 45 seconds in our recent tests. To make this process faster the use of electronic scanning can be the next alternative. A multiplexing system was developed as shown schematically in Figure 9, where a pair series of pitch-catch ultrasonic transducers was developed with the transducers directed toward a selected point on the top surface of the tested composite laminate. The data acquisition flow chart diagram is also shown in Figure 9 and the signals that are induced by the transmitter are received, processed and analyzed by a personal computer after being digitized. The developed software activates sequentially the various transducer pair to be triggered for data acquisition. Signals are induced by FM modulated function generator and are received by a set of receiver/amplifier after interrogating the test area. The function generator provides a reference frequency marker for calibration of the data acquisition when converting the signal from time to frequency domain. This multiplexed system of transducer pairs was also designed as an attachment added-on to ultrasonic C-scanners. The multiplexed transducer fixture is shown photographically in Figure 10.

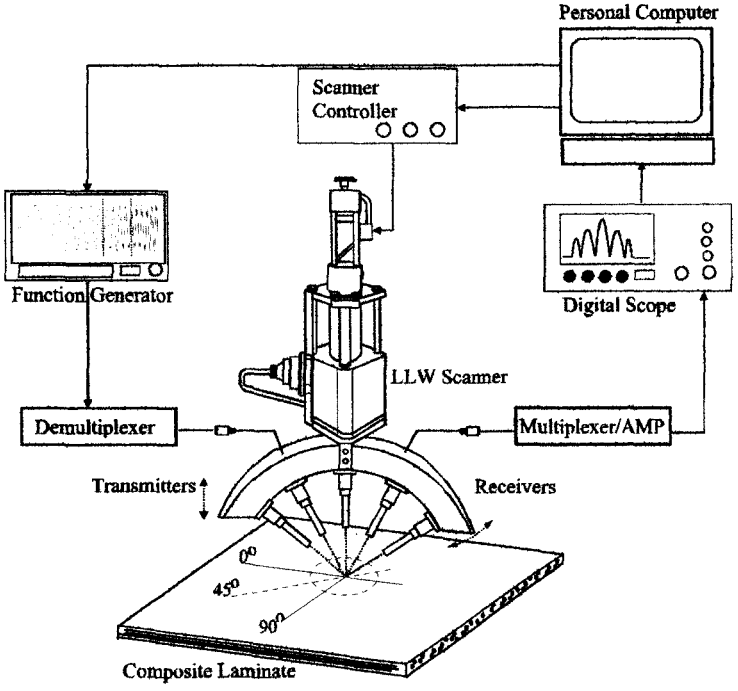


FIGURE 9: A schematic view of the multiple pairs of transducers system that are scanned electronic for testing composite material.

A system of 4 pairs of 5MHz transducers was used, which were aligned to transmit at 15, 30, 45 and 60 degrees angles of incidence. A multiplexer was designed to triggering the data acquisition of the selected transducer pair. The data acquisition setup consisted of a pulse generator HP 8116A, broadband receiver (Matec Model 605), amplifier (Panametrics Model 5052UA) and digital scope (LeCroy 9410 series dual 150 MHz oscilloscope). The digital scope displays the reflection spectrum in real time and a PC displays a user menu that controls the data acquisition and analysis operation. Further, the computer program was modified to automatically control the sequence of activated transducer pairs and the acquisition of the dispersion curve. Each pair represents a given angle of incidence and the acquired data is display on the screen. The computer marks the minima of the reflection spectrum (LLW modes) and the minima are

accumulated separately to form a dispersion curve. Once the dispersion data is ready, the software option of data inversion is activated and the elastic stiffness constants are determined.

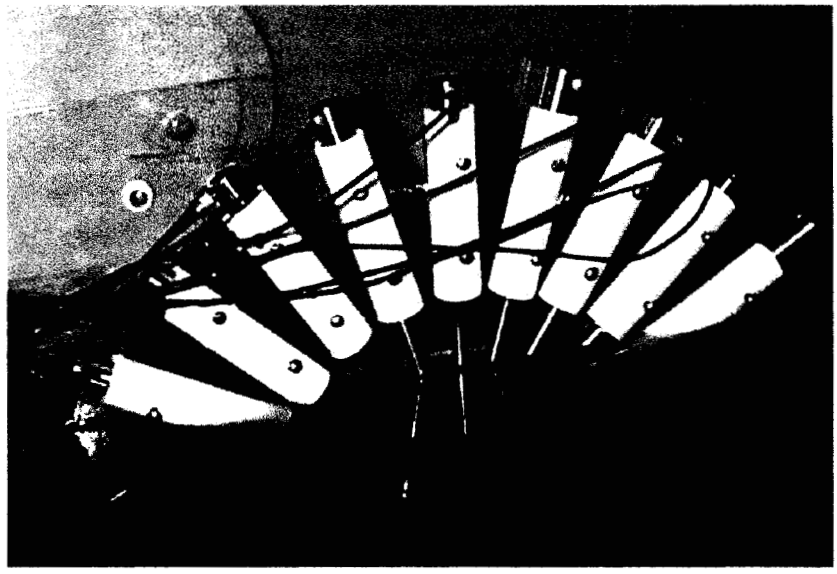

FIGURE 10: A view of the multi-probe system.

## ISSUES AFFECTING THE TRANSITION OF LLW TO PRACTICAL USE

The issues that affect the transition of the LLW method to standard NDE application include:

1. Material density - The inverted material constants assume that the material density is known. NDE measurement of the material density can be done by radiographic tests. However, such tests are not economical and they require access from two sides of the test structure, therefore an alternative method of measuring the density is needed.
2. Multi-orientation laminates - The inversion algorithm developed for the determination of the elastic properties has been very successful for unidirectional laminates. The analysis of laminates with multi-orientation layers using ply-by-ply analysis is complex and leads to ill-posed results. The authors are currently studying methods of inverting the material elastic properties without the necessity to deal with individual layers
3. Complex data acquisition - The LLW data acquisition setup is complex and the related process is not user friendly. The authors have significantly improved the data acquisition process, where a personal computer assists the user by optimizing the setup height to assure the greatest ratio between the maximum and minimum amplitudes in the reflected spectrum. The polar angle is set using the polar backscattering technique [Bar-Cohen and Crane, 1982] to determine the direction of the first layer. Further, user friendly control software that operates on the Widows platform is being developed to allow interactive software control.
4. Time-consuming process - The formerly reported process of acquiring a dispersion curve was time consuming and took between 10 and 20 minutes to acquire a curve for a single point on the composite material. Recent development by the authors allows the measurement of the dispersion curves at a significantly higher speed in the range of fraction of a minute. Using the new capability of rapid acquisition, various defects can be detected and characterized based on their dispersion curve data. This increased speed of dispersion data acquisition offers the capability to produce C-scan images where variations in individual stiffness constants can be mapped.

## CONCLUSIONS

The leaky Lamb wave (LLW) method has been studied by numerous investigators who contributed significantly to the understanding of wave behavior in anisotropic materials. However, in spite of this progress, the LLW method is still far from being an acceptable standard NDE method. The authors investigated the potential issues that are hampering this transition to practical NDE and identified 4 key issues: a) There is a need to determine the density nondestructively using access from a single-side; b) The technique should be applicable to multi-layer angle-ply composites; c) The data acquisition process needs to be more user friendly; and d) The process of data acquisition needs to be more rapid. The authors have made significant progress in the simplification of the data acquisition process and the acquisition speed with some progress has been made in dealing with cross-ply and quasi-isotropic laminates. The inability to measure the material density with an NDE tool using access from a single side of a laminate is still considered an unresolved issue and will require further research.

## ACKNOWLEDGMENT

The research at Jet Propulsion Laboratory (JPL), California Institute of Technology, was carried out under a contract with National Aeronautics Space Agency (NASA), and the research at UCLA under AFOSR grant F49620-93-1-0320. Further, the authors would like to thank Ms. Sue Kersey, Mr. Cedric Daksla and Mr. Anatoly Blanovsky who assisted in developing the multiplexed LLW scanner, during their M.S. thesis studies at the UCLA Integrated Manufacturing Engineering Department. Also, the author would like to thank Mr. Hamid Kohen, a UCLA graduate student specializing in artificial intelligence, for his investigation of the LLW mode images using Canning Filter.

## RERFERENCES

Bar-Cohen, Y., and R. L. Crane, "Acoustic-Backscattering Imaging of Subcritical Flaws in Composites," Materials Evaluation, Vol. 40, No. 9 (1982), pp. 970-975.

Bar-Cohen, Y., and D.E. Chimenti, Review of Progress in Quantitative NDE, Vol. 3B, D. O. Thompson & D.E. Chimenti (Eds.), Plenum Press, New York and London (1984), pp. 1043-1049.

Bar-Cohen, Y., A.K. Mal and C. -C. Yin, Journal of Adhesion, Vol. 29, No. 1-4, (1989), pp. 257-274.

Bar-Cohen, Y., et al, "Ultrasonic Testing Applications in Advanced Materials & Processes," Nondestructive Testing Handbook, Section 15 in Vol. 7: Ultrasonic Testing, Section 8, A. Birks and B. Green Jr. (Ed.), American Society for NDT, Columbus, OH (1991) pp. 514-548.

Bar-Cohen, Y., A. Mal, and S.-S. Lih, "NDE of Composite Materials Using Ultrasonic Oblique Insonification, Materials Evaluation, Vol. 51, No. 11, (1993), pp.1285-1295.

Bar-Cohen, Y., P. Backes, "Multifunction Automated Crawling System (MACS)," Proceedings of the SPIE, Vol. 2945, NDE of Aging, Airports and Aerospace Hardware, Dec. 2-5, 1996, pp. 74-77.

Buchwald, V. T., "Rayleigh Waves in Transversely Isotropic Media," Quarterly J. Mechanics and Applied Mathematics, Vol. 14 (1961) pp. 293-317.

Christensen, R. M., "Mechanics of Composite Materials," Chapter 4, Wiley, New York (1981).

Dayal, V., and V.K. Kinra, J. Acoustic Soc. of Amer., Vol. 89, No. 4 (1991), pp. 1590-1598.

Mal, A. K., "Wave Propagation in Layered Composite Laminates under Periodic Surface Loads." Wave Motion, Vol. 10, (1988), PP. 257-166.

Mal, A. K., and Y. Bar-Cohen, Proceedings of the Joint ASME and SE meeting, AMD-Vol. 90, A. K. Mal and T.C.T. Ting (Eds.), ASME, NY, (1988), pp. 1-16.
Mal, A. K., C. -C. Yin, and Y. Bar-Cohen, "Ultrasonic NDE of Cracked Composite Laminates," Composites Engineering, Pergamon Press, Vol. 1, No. 2, (1991), pp. 85-101.
Nayfeh, A. H., and D. E. Chimenti, J. Applied Mechanics, Vol. 55 (1988) p. 863.